Synthesis and Structural Characterisation of Ag^{I} Complexes with *N*,*N*′-Bis(2-pyridyl)oxalamide and the Anion of *N*-(2-Pyridyl)oxalamic Acid

Hui-Ling Hu,[a] Chun-Wei Yeh,[b] and Jhy-Der Chen*[b]

Keywords: Silver / Coordination polymer / *N*-(2-Pyridyl)oxalamic acid / *N*,*N*-Bis(2-pyridyl)oxalamide

A series of silver(I) complexes of the type $\{[Ag_2(\mathbf{L})_2(\mathbf{L}')][X]\}_\infty$ [**L** = *N*,*N*′-bis(2-pyridyl)oxalamide; **L**′ = anion of *N*-(2-pyridyl)-oxalamic acid; X = BF_4^- (**1**), ClO_4^- (**2**), PF_6^- (**3**) and NO_3^- (**4**)] have been prepared from the reaction of AgX with **L** in $EtOH/H_2O$. All the complexes have been structurally characterised by X-ray crystallography confirming that complexes **1**–**4** are 2D coordination polymers. The Ag^{I} centres show two types of coordination geometries, i.e. distorted trigonal-bipyramidal and distorted tetrahedral which are linked by the **L** and **L**′ ligands, forming unique 2D doubly pleated rectangular grids. The anions BF_4^-, ClO_4^- and PF_6^- in complexes **1**–**3** are not coordinated to the Ag^{I} centres whereas the NO_3^- anions in **4** are coordinated to the metal centres through one of the three oxygen atoms. The transformation of **L** to **L**′ is also discussed.

Introduction

Recently, a great deal of effort has been devoted to the self-assembly of organic and inorganic molecules in the solid state because it extends the range of new solids which can be designed to have particular physical and chemical properties.[1,2] The range and variety of self-assembling inorganic structures that can be constructed relies on the presence of suitable metal−ligand interactions and supramolecular contacts, i.e., hydrogen bonds and other weak interactions.[3] Many topologically promising Ag^{I}-containing architectures have been constructed with bidentate building blocks containing nitrogen donors.[4] The polymers include 1D, 2D and 3D network structures.[4b]

In our continuing work on the preparation of complexes with new structural types,[5] we have reported[5b] a series of 1D coordination polymers, $\{[Ag(\mathbf{L})][NO_3]\}_\infty$, $\{[Ag(\mathbf{L})(CH_3CN)][ClO_4]\}_\infty$, $\{[Ag_2(\mathbf{L})_3(CH_3CN)_2][PF_6]_2\}_\infty$ and $[Ag_3(\mathbf{L})_4(CH_3CN)_4][BF_4]_3$ which were prepared by the reaction between AgX (X = NO_3^-, ClO_4^-, PF_6^- and BF_4^-) and the bidentate ligand *N*,*N*′-bis(2-pyridyl)oxalamide (**L**) in CH_3CN.

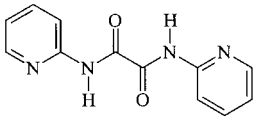

L

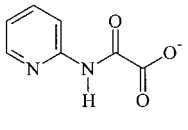

L'

[a] Department of Chemical Engineering, Nanya Institute of Technology,
Chung-Li, Taiwan, R.O.C.
[b] Department of Chemistry, Chung-Yuan Christian University, Chung-Li, Taiwan, R. O. C.

These complexes are capable of self-assembling into 2D molecular structures through a series of interactions involving Ag−O weak covalent bonds and self-complementary double N−H···O hydrogen bonds.[5b] It was also found that changing the counterion had a drastic effect on the structures of the Ag^{I} coordination polymers. Interestingly, when the reactions were carried out in $EtOH/H_2O$, transformation of the **L** ligand to the anion of *N*-(2-pyridyl)oxalamic acid (**L**′) was observed and the Ag^{I} ions were interlinked by both of the **L** and **L**′ ligands forming unique 2D doubly pleated rectangular grids. The syntheses and structural characterisation of complexes of the type $\{[Ag_2(\mathbf{L})_2(\mathbf{L}')][X]\}_\infty$ [**L** = *N*,*N*′-bis(2-pyridyl)oxalamide]; **L**′ = anion of *N*-(2-pyridyl)oxalamic acid; X = BF_4^-, ClO_4^-, PF_6^- and NO_3^-) form the subject of this report.

Results and Discussions

Syntheses

Complexes of the type $\{[Ag_2(\mathbf{L})_2(\mathbf{L}')][X]\}_\infty$ [**L** = *N*,*N*′-bis(2-pyridyl)oxalamide; **L**′ = anion of *N*-(2-pyridyl)oxalamic acid; X = BF_4^- (**1**), ClO_4^- (**2**), PF_6^- (**3**) and NO_3^- (**4**)] have been prepared by the reaction of AgX with **L** in $EtOH/H_2O$. The IR spectra show broad bands in the range from 3160 to 3184 cm^{-1} for complexes **1**−**4**, assignable to the N−H stretching vibrations. Two strong absorption bands at 1702 and 1685 cm^{-1} were observed for each of the complexes **1**−**4** which can be assigned to the C=O stretching of **L**′ and **L**, respectively. For complexes **1**−**4**, the IR spectra also exhibit strong bands at 1593−1595 cm^{-1} due

  DOI: 10.1002/ejic.200400101

to the $\nu_{as}(COO^-)$ mode in addition to the other strong bands at 1304−1305 cm^{-1} associated with the $\nu_s(COO^-)$ mode which are consistent with the coordination of the carboxylate groups in these complexes. The formation of the carboxylate groups indicates the transformation of **L** to **L′** which was verified by their X-ray crystallographic structures.

The yields of the products were fully dependent on the length of time of crystallisation. Attempts to shorten the time by stirring or heating the reactants to reflux always led to the formation of a mixture of several compounds which, due to their insolubilities in common solvents, could not be separated. Preparation of the four complexes using solutions of **L** and **L′** in nonaqueous media in a 1:1 ratio is one of our research projects currently under investigation. Instead of **L′**, we have attempted several reactions using ligands such as **L** and nicotinic acid (Hnic) in CH_3OH or ethanol solution, but only a mixture of Ag(nic) and Ag(**L**)(X) was obtained.

Differential scanning calorimetry (DSC) experiments of complexes **1**−**4** show endothermic peaks in the curves and the values of the melting temperatures (T_m) for complexes **1**−**4** are 216.21, 215.65, 214.88 and 215.78 °C, respectively. These results indicate that the stabilities of the network structures of complexes **1**−**4** are similar and are not dependent one the nature of the anions.

Structures of Complexes 1−4

The crystal structures of complexes **1**−**4** belong to the space group *Pnma*. A representative asymmetric unit and ORTEP diagrams showing the geometries of Ag(1) and Ag(2) in complexes **1**−**3** are depicted in Figure 1 (a, b, and c, respectively), while the asymmetric unit and ORTEP diagram showing the geometry about Ag(2) in complex **4** are shown in Figure 2 (a and b, respectively). The geometry about Ag(1) in complex **4** is shown in Figure 2 (b). Tables 1 and 2 list the bond lengths and angles around Ag(1) and Ag(2), respectively, for complexes **1**−**4**. Two types of coordination geometries are observed for the metal centres. The Ag(1) atom which is coordinated by two pyridyl nitrogen atoms of different **L** ligands, one pyridyl nitrogen atom of **L′** and one carboxylate oxygen atom and one carbonyl oxygen atom of the same **L′** is distorted trigonal-bipyramidal. The Ag(2) atom which is coordinated by two pyridyl nitrogen atoms of different **L** ligands and the two carboxylate oxygen atoms of the **L′** ligand is distorted tetrahedral. The structural difference between complexes **1**−**3** and **4** is that the anions in **1**−**3** link the metal centres through weak interactions while the NO_3^- anion in complex **4** coordinates to the metal centre through its oxygen atom [Ag(2)−O(6): 2.494(8) Å]. It can be seen form Tables 1 and 2 that the Ag−N distances to the Ag(1) atoms are all similar, while that to the Ag(2) atom in complex **4**, which is 2.432(4) Å, is significantly longer than those in the other three complexes. The Ag(1)−O distances to the carbonyl oxygen atoms of the **L′** ligand are all longer than those to the carboxylate oxygen atoms, while the Ag(2)−O distances in complexes **1**−**3** are all similar. The bond angles around the Ag(1) centres are normal for a distorted trigonal-bipyramidal geometry. Due to the chelation of the aceto group of the **L′** ligand, the O−Ag(2)−O angles for complexes **1**−**3** are 51.8(2), 51.6(3) and 52.05(19)°, respectively, while the other O−Ag−N and N−Ag−N angles are in the range from 103.0(2) to 127.0(2)°.

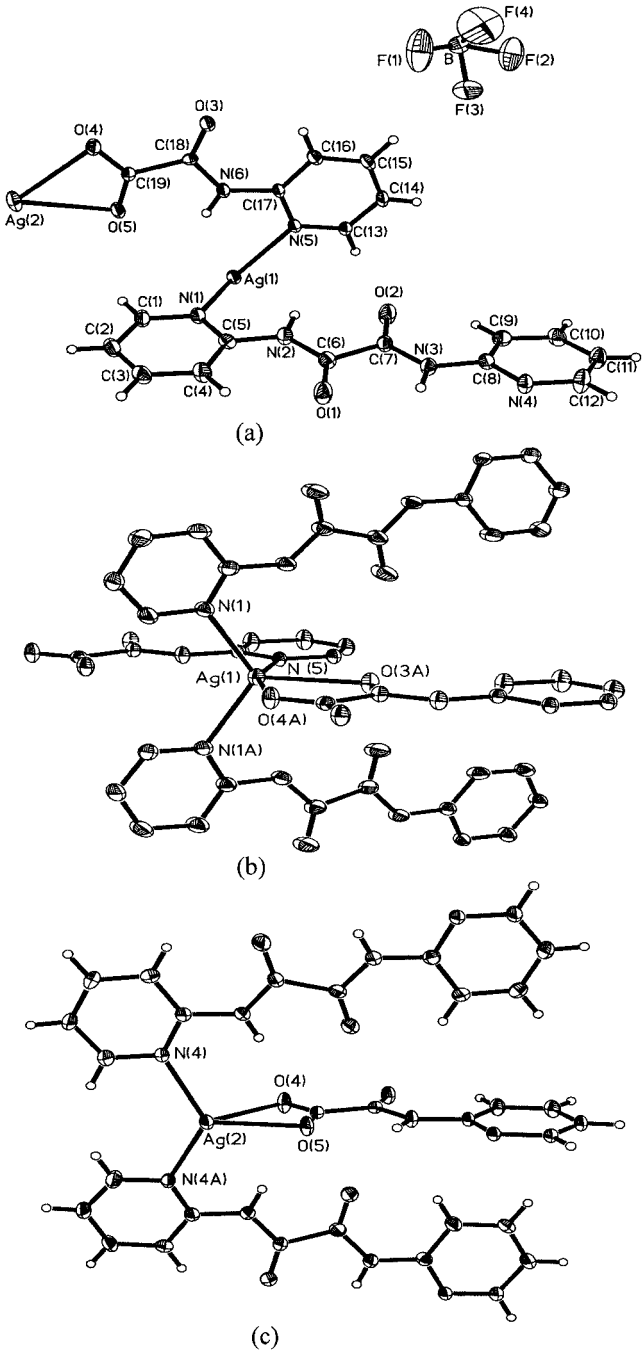

Figure 1. (a) Representative asymmetric unit of the cation in **1**−**3**; (b) ORTEP diagram showing the arrangement around Ag(1); (c) ORTEP diagram showing the arrangement around Ag(2)

The most remarkable feature of complexes **1**−**4** is that they are coordination polymers of $[Ag_2(\mathbf{L})_2(\mathbf{L}')][X]$, forming 2D doubly pleated rectangular grids (Figure 3, bot-

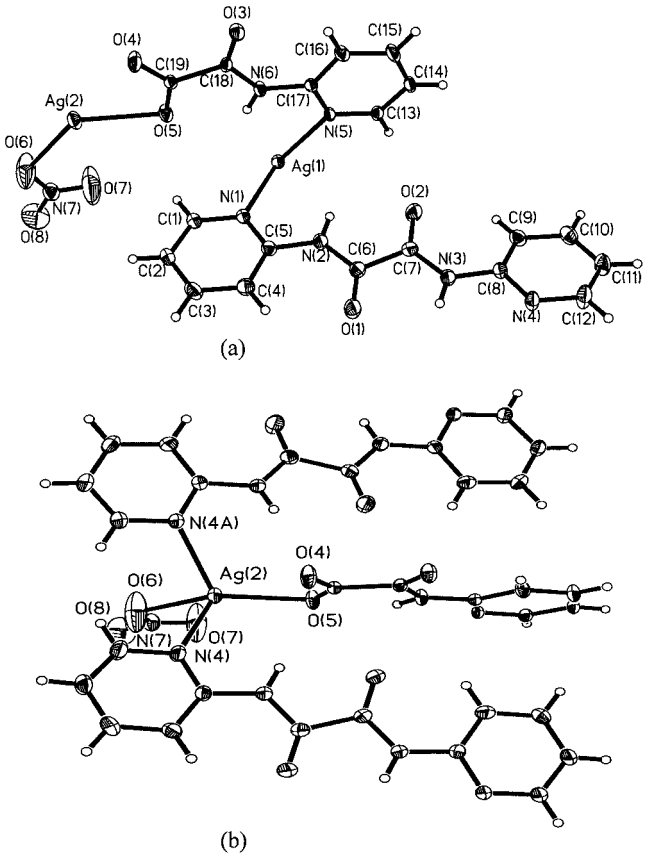

Figure 2. (a) Asymmetric unit of **4**; (b) ORTEP diagram showing the arrangement around Ag(2)

Table 1. Bond lengths [Å] and angles [°] around the Ag(1) centres for complexes **1**−**4**

	1	**2**	**3**	**4**
Distances:				
Ag(1)−N(5)	2.329(6)	2.327(9)	2.301(6)	2.372(4)
Ag(1)−N(1)	2.406(5)	2.410(6)	2.454(5)	2.394(3)
Ag(1)−O(3A)	2.524(6)	2.542(8)	2.551(6)	2.509(4)
Ag(1)−O(4A)	2.384(6)	2.379(8)	2.360(6)	2.415(4)
Angles:				
N(5)−Ag(1)−N(1)	105.85(14)	104.53(19)	104.03(13)	105.62(9)
N(5)−Ag(1)−O(4A)	158.2(2)	158.8(3)	159.6(2)	158.39(15)
N(5)−Ag(1)−O(3A)	89.8(2)	90.2(3)	91.4(2)	89.52(13)
N(1)−Ag(1)−O(3A)	114.50(14)	115.25(17)	114.70(12)	119.78(16)
N(1)−Ag(1)−N(1B)	120.6(2)	120.6(3)	121.5(2)	
O(4A)−Ag(1)−O(3A)	68.4(2)	68.5(3)	68.15(19)	68.86(13)
N(1)−Ag(1)−O(4B)				84.59(10)
N(1)−Ag(1)−O(4B)				89.59(10)
O(4A)−Ag(1)−N(1)	84.27(15)	85.5(2)	85.45(14)	

Symmetry transformations used to generate equivalent atoms: A: x, $-y + 1/2$, z; B: x, y, $z + 1$.

tom, for complexes **1**−**3**, while that of **4** is shown in Figure 4). The 2D doubly-pleated-grid structure can be regarded as interweaving of concavo-convex chains involving **L** ligands and zigzag chains involving **L′** ligands, as shown in Figure 3, top and center, respectively. The **L** ligand coordinates to the metal centres in a bidentate fashion through

Table 2. Bond lengths [Å] and angles [°] around the Ag(2) centres in complexes **1**−**4**

	1	**2**	**3**	**4**
Distances:				
Ag(2)−O(4)	2.535(6)	2.552(8)	2.495(6)	2.723
Ag(2)−O(5)	2.480(6)	2.463(8)	2.522(6)	2.428(4)
Ag(2)−O(6)				2.494(8)
Ag(2)−N(4C)	2.301(5)	2.300(7)	2.285(5)	2.432(4)
Angles:				
N(4C)−Ag(2)−N(4D)	124.7(2)	123.4(3)	127.0(2)	116.96(17)
N(4C)−Ag(2)−O(4)	104.50(15)	103.0(2)	108.50(13)	
N(4C)−Ag(2)−O(5)	117.52(12)	117.83(16)	116.29(12)	
O(5)−Ag(2)−O(4)	51.8(2)	51.6(3)	52.05(19)	128.5(2)
N(4C)−Ag(2)−O(6)				87.44(13)
O(5)−Ag(2)−N(4C)				115.83(8)
O(5)−Ag(2)−N(6)				128.5(2)

Symmetry transformations used to generate equivalent atoms: C: $-x$, $-y$, $-z + 2$; D: $-x$, $y + 1/2$, $-z + 2$.

the two pyridyl nitrogen atoms, while the **L′** ligand chelates and bridges three Ag^I atoms in a tetradentate bonding mode through all the three oxygen atoms and the pyridyl nitrogen atom. A schematic drawing of the 2D structures of complexes **1**−**4** is shown in Figure 5, where the Ag^I ions occupy the intersections. Two types of rectangles with the same lengths and different widths can be found for complexes **1**−**4** and Table 3 lists the sizes for these rectangles. The dihedral angles between the adjacent rectangles are listed in Table 4. It can be seen from Tables 3 and 4 that the sizes and dihedral angles for complexes **1**−**4** are similar, although slight differences have been found for complex **4**, indicating that changing the anions hardly affects the structures of the cations. Such a type of grid is unique and is in marked contrast to the regular grids found previously.[6] This 2D structure is also in marked contrast to our reported Ag^I complexes containing *N*,*N′*-bis(2-pyridyl)oxalamide ligands, where only 1D coordination polymers were obtained.[5b]

In complexes **1**−**4**, the 2D grids are further linked by the anions through Ag···X interactions (X = F or O) and/or C−H···X hydrogen bonds to form 3D structures (Ag···F−B 2.981, 3.070 Å, C−H···F−B 2.492−2.559 Å for **1**; Ag···O−Cl 2.926, 2.919 Å, C−H···O−Cl 2.528−2.580 Å for **2**; Ag···F−P 3.065−3.611 Å, C−H···F−P 2.405−2.527 Å for **3**; C−H···O−N 2.434 Å for **4**). Figure 6 shows a representative packing diagram for **2**. It can be seen that the molecules pack into layers of 2D cations which are separated by layers of the anions.

Transformation of L to L′

As shown in the structures of complexes **1**−**4**, a transformation of **L** to **L′** was observed. There are three possible reasons for this transformation. (1) The formation of **L′** could be due to the contamination of the by-product, *N*-(2-pyridyl)oxalamic acid, which may have been formed during the preparation of **L**. This possibility can be ruled out since all the spectroscopic data of **L** show that the ligand is pure

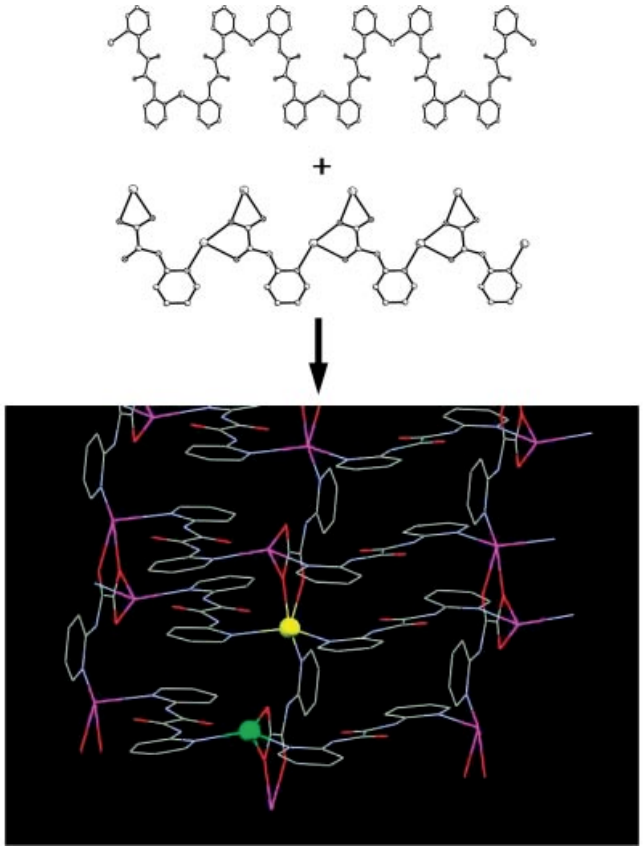

Figure 3. ORTEP drawings showing the concavo-convex chain involving **L** ligands (top), zigzag chain involving **L**′ ligands (center) and the 2D structure looking down the *a* axis (bottom)

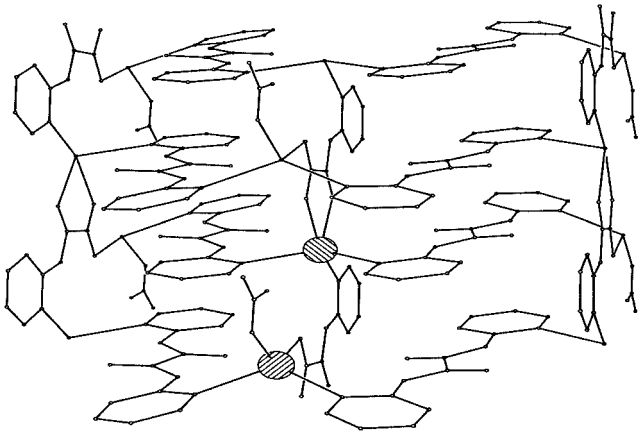

Figure 4. 2D structure of **4**

with no contamination of *N*-(2-pyridyl)oxalamic acid. (2) The **L** ligand decomposes to form *N*-(2-pyridyl)oxalamic acid during the crystallisation of complexes **1**−**4** in EtOH/H_2O. A blank test without addition of the metal salts had been carried out and no indication of *N*-(2-pyridyl)oxalamic acid was observed even under continuous stirring for more than two months. (3) The transformation is thus due to catalysis by Ag^+ in EtOH/H_2O. This shows that the metal centre plays an important role in converting **L** to **L**′.

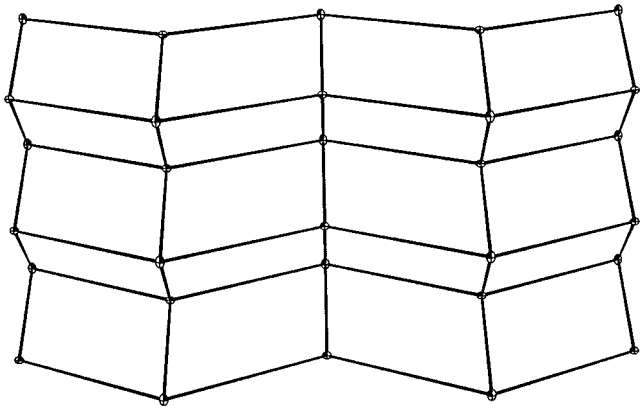

Figure 5. Schematic drawing for complexes **1**−**4**

Table 3. The sizes [Å] of small and large rectangles for complexes **1**−**4**

Complex	Small		Large	
	Length	Width	Length	Width
1	9.537	4.751	9.537	6.162
2	9.537	4.768	9.537	6.160
3	9.637	4.660	9.637	6.338
4	9.612	5.023	9.612	5.984

Table 4. Dihedral angles [°] between rectangles for complexes **1**−**4**

Complex	Large & large	Large & small	Small & small
1	37.7	86.1	48.9
2	39.1	86.1	47.7
3	38.2	86.3	47.2
4	40.7	85.9	48.4

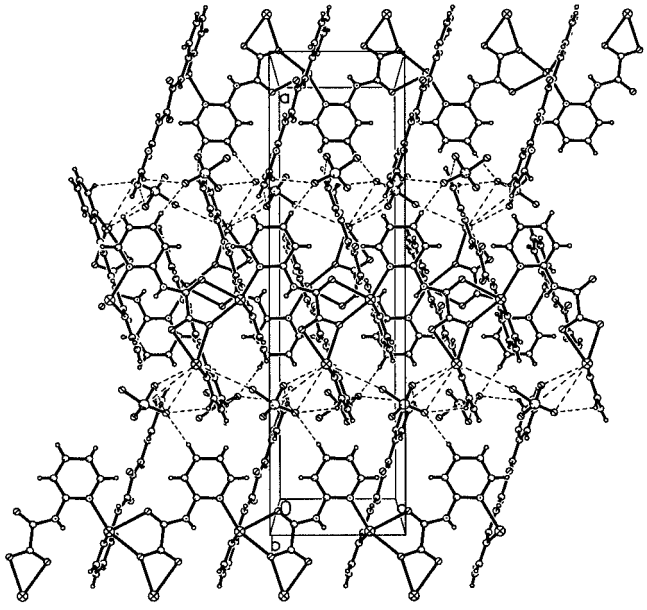

Figure 6. Packing diagram for **2** showing the interactions between the cations and the anions

Stronger Lewis acids such as $AlCl_3$ have been used to investigate the conversion, but no positive results could be obtained. A mechanism describing the transformation pathways of **L** to **L′** is proposed in Scheme 1. The Ag^+ first coordinates to the carbonyl oxygen atom of **L′** followed by nucleophilic attack of a water molecule on the carbonyl carbon atom. A 2-aminopyridinium cation is lost to give Ag**L′** which then reacts with another **L** to afford complexes **1**−**4**.

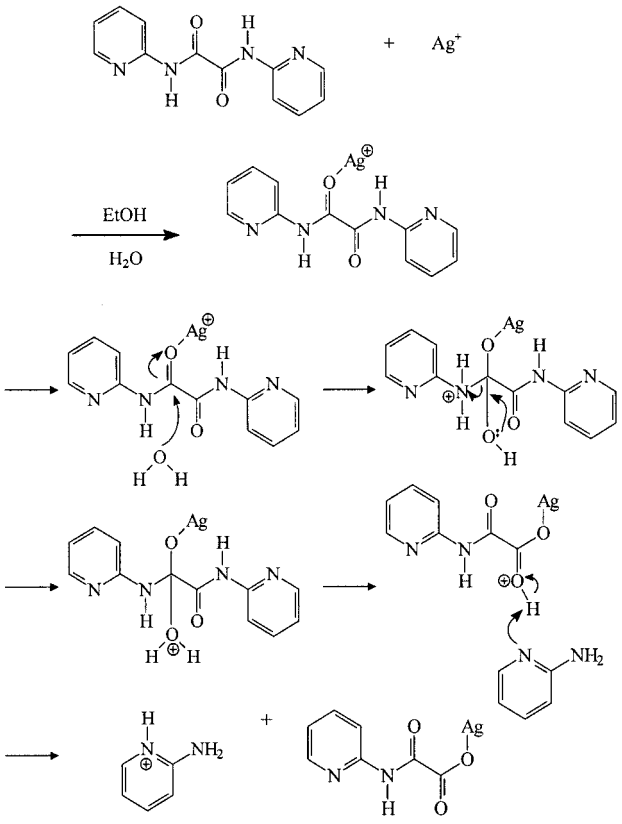

Scheme 1. Mechanism showing the transformation of **L** to **L′**

Concluding Remarks

In this study, the coordination chemistry of AgX (X = BF_4^-, ClO_4^-, PF_6^- and NO_3^-) with *N*,*N*′-bis(2-pyridyl)oxalamide (**L**) and the anion of *N*-(2-pyridyl)oxalamic acid (**L′**) was investigated. Unique 2D doubly-pleated-grid structures were seen in these complexes. During the crystallisation of the complexes, some of the **L** ligands were transformed to **L′** in the presence of Ag^I ions and water molecules. It has also been shown that the 2D pleated grids adopted by complexes **1**−**4** were hardly altered upon changing their counterions.

Experimental Section

General Procedures: All manipulations were carried out under air. The visible absorption spectra were recorded with a Hitachi U-2000 spectrophotometer. IR spectra were obtained with a Jasco FT/IR-460 plus spectrometer. Elemental analyses were obtained with a PE 2400 series II CHNS/O analyser or a HERAEUS VaruoEL analyser.

Materials: The reagents AgX (X = BF_4^-, ClO_4^-, PF_6^- and NO_3^-) were purchased from Aldrich Chemical Co. The ligand *N*,*N*′-bis(2-pyridyl)oxalamide was prepared according to a literature procedure.[7]

Syntheses: The complexes were synthesised by treatment of AgX (X = BF_4^-, ClO_4^-, PF_6^- and NO_3^-) with *N*,*N*′-bis(2-pyridyl)oxalamide in EtOH/H_2O.

1: *N*,*N*′-Bis(2-pyridyl)oxalamide (0.048 g, 0.20 mmol) in EtOH (5 mL) was layered onto a solution of $AgBF_4$ (0.020 g, 0.10 mmol) in H_2O (5 mL). The resultant solution was allowed to slowly diffuse for several weeks to give colourless crystals. Yield: 0.013 g, (27.0%). $C_{31}H_{27}Ag_2BF_4N_{10}O_8$ (**1**·H_2O; 970.16): calcd. C 38.38, H 2.81, N 14.44; found C 38.19, H 2.46, N 14.28. IR (KBr disk, cm^{-1}): $\tilde{\nu}$ = 3446 (w), 3172 [br., ν_s(N−H)], 1702 [s, ν_s(C=O)], 1685 [s, ν_s(C=O)], 1593 [br., $\nu_{as}(COO^-)$ + ν(C=N)], 1576 (s), 1499 (s), 1434 (s), 1305 [s, $\nu_s(COO^-)$], 1084 (w), 777 (m), 626 (w), 551 (w), 484 (w).

2: Prepared as described for **1**. Yield 0.015 g (28%). $C_{31}H_{27}Ag_2ClN_{10}O_{12}$ (**2**·H_2O; 982.80): calcd. C 37.89, H 2.77, N 14.25; found C 37.90, H 2.65, N 14.33. IR (KBr disk, cm^{-1}): $\tilde{\nu}$ = 3410 (w), 3180 [br., ν_s(N−H)], 1702 [s, ν_s(C=O)], 1685 [s, ν_s(C=O)], 1593 [br., $\nu_{as}(COO^-)$ + ν(C=N)], 1575 (s), 1498 (s), 1434 (s), 1305 [s, $\nu_s(COO^-)$], 1145 (s, ClO_4^-), 777 (m), 627 (w), 551 (w), 484 (w).

3: Prepared as described for **1**. Yield: 0.016 g (31%). $C_{31}H_{27}Ag_2F_6N_{10}O_8P$ (**3**·H_2O; 1028.32): calcd. C 36.21, H 2.65, N 13.62; found C 35.92, H 2.49, N 13.43. IR (KBr disk, cm^{-1}): $\tilde{\nu}$ = 3412 (w), 3160 (br., ν_s(N−H)], 1702 [s, ν_s(C=O)], 1685 [s, ν_s(C=O)], 1595 (br., $\nu_{as}(COO^-)$ + ν(C=N)], 1576 (s), 1498 (s), 1433 (s), 1304 [s, $\nu_s(COO^-)$], 837 (w), 770 (m), 626 (w), 551 (w), 483 (w).

4: Prepared as described for **1**. Yield: 0.013 g (28%). $C_{31}H_{27}Ag_2N_{11}O_{10}$ (**4**·H_2O; 929.36): calcd. C 40.06, H 2.93, N 16.58; found C 39.26, H 2.60, N 16.51. IR (KBr disk, cm^{-1}): $\tilde{\nu}$ = 3422 (w), 3184 [br., ν_s(N−H)], 1702 [s, ν_s(C=O)], 1685 [s, ν_s(C=O)], 1595 [br., $\nu_{as}(COO^-)$ + ν(C=N)], 1575 (s), 1498 (s), 1433 (s), 1384 (s, NO_3^-), 1304 [s, $\nu_s(COO^-)$], 770 (m), 626 (w), 551 (w), 483 (w).

X-ray Crystallography: The diffraction data of **1** were collected with a Bruker AXS diffractometer using graphite-monochromated Mo-K_α (K_α = 0.71073 Å) radiation. Data reduction was carried out using standard methods with the use of well-established computational procedures.[8] The structure factors were obtained after Lorentz and polarisation corrections. The positions of the heavy atoms, including the silver atoms, were located by direct methods. The remaining K_α (K_α = 0.71073 Å) radiation. Data reduction was carried out using and least-squares refinements.[9] The final residuals were R_1 = 0.0514, $wR2$ = 0.1309. The crystallographic procedures for **2**−**4** were similar to those for **1**. Basic information pertaining to crystal parameters and the structure refinements is summarized in Table 5. CCDC-230419 to -230422 contain the supplementary crystallographic data for this paper. These data can be obtained free of charge at www.ccdc.cam.ac.uk/conts/retrieving.html [or from the Cambridge Crystallographic Data Centre, 12 Union Road, Cambridge, CB2 1EZ, UK; Fax: (internat.) + 44-1223-336-033; E-mail: deposit@ccdc.cam.ac.uk].

Table 5. Crystal data for compounds **1**−**4**

	1	**2**	**3**	**4**
Empirical formula	$C_{31}H_{25}Ag_2BF_4N_{10}O_7$	$C_{31}H_{25}Ag_2ClN_{10}O_{11}$	$C_{31}H_{25}Ag_2F_6N_{10}O_7P$	$C_{31}H_{25}Ag_2N_{11}O_{10}$
Formula mass	952.16	964.8	1010.32	927.36
Crystal system	orthorhombic	orthorhombic	orthorhombic	orthorhombic
Space group	*Pnma*	*Pnma*	*Pnma*	*Pnma*
a [Å]	27.469(2)	27.453(3)	27.884(3)	27.227(3)
b [Å]	16.426(2)	16.532(2)	16.681(2)	16.251(2)
c [Å]	7.4868(7)	7.511(2)	7.5763(12)	7.4935(7)
V [Å^3]	3378.0(6)	3409(1)	3523.9(8)	3315.6(5)
Z	4	4	4	4
$d_{calcd.}$ [gcm^{-3}]	1.872	1.897	1.904	1.823
Crystal size [mm]	0.1 × 0.2 × 0.7	0.1 × 0.2 × 0.4	0.1 × 0.2 × 0.8	0.1 × 0.2 × 0.7
μ(Mo-K_α) [mm^{-1}]	1.247	1.317	1.253	1.235
Temp. [°C]	22	22	22	22
Data/restraints/parameters	3057/0/289	3093/0/289	3200/0/338	3015/0/271
Quality-of-fit indicator[a]	1.048	1.005	1.012	1.013
Final *R* indices [$I > 2\sigma(I)$][b] [c]	$R_1 = 0.0514, wR_2 = 0.1309$	$R_1 = 0.0609, wR_2 = 0.1255$	$R_1 = 0.0496, wR_2 = 0.1236$	$R_1 = 0.0370, wR_2 = 0.0867$
R indices (all data)	$R_1 = 0.0691, wR_2 = 0.1422$	$R_1 = 0.1311, wR_2 = 0.1562$	$R_1 = 0.0703, wR_2 = 0.1389$	$R_1 = 0.0531, wR_2 = 0.0952$

[a] Quality-of-fit = $\{[\Sigma w||F_o^2| - |F_c^2||^2/N_{observed} - N_{parameters}]\}^{1/2}$. [b] $R_1 = \Sigma||F_o| - |F_c||/\Sigma|F_o|$. [c] $wR_2 = [\Sigma w(F_o^2 - F_c^2)^2/\Sigma w(F_o^2)^2]^{1/2}$. $w = 1/[\sigma^2(F_o^2) + (ap)^2 + (bp)]$, $p = [\max.(F_o^2 \text{ or } 0) + 2(F_c^2)]/3$. $a = 0.0694$, $b = 11.5112$ for **1**; $a = 0.0757$, $b = 0$ for **2**; $a = 0.0747$, $b = 8.7532$ for **3**; $a = 0.0482$, $b = 2.8985$ for **4**.

Acknowledgments

We are grateful to the National Science Council of the Republic of China for support.

[1] [1a] G. R. Desiraju, *Angew. Chem. Int. Ed. Engl.* **1995**, *34*, 2311−2327. [1b] G. R. Desiraju, *Chem. Commun.* **1997**, 1475−1482. [1c] J. M. Lehn, *Supramolecular Chemistry*, Wiley-VCH, Weinheim, **1995**.

[2] [2a] R. Robson, B. E. Abrahams, S. R. Batten, R. W. Gable, B. F. Hoskins, J. Lieu, *Supramolecular Architecture*, ACS publications, Washington, DC, **1992**. [2b] S. R. Batten, R. Robson, *Angew. Chem. Int. Ed.* **1998**, *37*, 1460−1494. [2c] O. M. Yaghi, H. Li, C. Davis, D. Richardson, T. L. Groy, *Acc. Chem. Res.* **1998**, *31*, 474−484. [2d] H. Gudbjartson, K. Biradha, K. M. Poirier, M. J. Zaworotko, *J. Am. Chem. Soc.* **1999**, *121*, 2599−2600. [2e] C. B. Aakeröy, K. R. Seddon, *Chem. Soc., Rev.* **1993**, 397−407. [2f] M. Fujita, K. Ogura, *Coord. Chem. Rev.* **1996**, *148*, 249−264. [2g] S.-I. Noro, R. Kitauta, M. Kondo, S. Kitagawa, T. Ishii, H. Matauzaka, M. Yamashita, *J. Am. Chem. Soc.* **2002**, *124*, 2568−2583. [2h] S. Kitagawa, M. Kondo, *Bull. Chem. Soc. Jpn.* **1998**, *71*, 1739−1753.

[3] [3a] R. P. Sijbesma, E. W. Meijer, *Curr. Opin. Colloid Interface Sci.* **1999**, *4*, 24−32. [3b] S. C. Zimmerman, P. S. Corbin, *Struct. Bonding* **2000**, *96*, 63−94. [3c] D. C. Sherrington, K. A. Taskinen, *Chem. Soc. Rev.* **2001**, *30*, 83−93. [3d] D. S. Lawrence, T. Jiang, M. Levett, *Chem. Rev.* **1995**, *95*, 2229−2260.

[4] [4a] A. J. Blake, N. R. Champness, P. Hubberstey, W.-S. Li, M. A. Withersby, M. Schröder, *Coord. Chem. Rev.* **1999**, *183*, 117−138. [4b] S. Muthu, J. H. K. Yip, J. J. Vittal, *Dalton Trans.* **2002**, 4561−4568, and references cited therein.

[5] [5a] C.-W. Su, C.-P. Wu, J.-D. Chen, L.-S. Liou, J.-C. Wang, *Inorg. Chem. Commun.* **2002**, *5*, 215−219. [5b] Y.-F. Hsu, J.-D. Chen, *Eur. J. Inorg. Chem.* **2004**, 1488−1493.

[6] [6a] S.-L. Zheng, M.-L. Tong, X.-L. Yu, X.-M. Chen, *J. Chem. Soc., Dalton Trans.* **2001**, 586−592. [6b] M. J. Zaworotko, *Chem. Commun.* **2001**, 1−9. [6c] J. Y. Lu, K. A. Runnels, C. Norman, *Inorg. Chem.* **2001**, *40*, 4516−4517. [6d] M. J. Plater, M. R. St J. Foreman, A. M. Z. Slawin, *J. Chem. Research (S)* **1999**, 74−75. [6e] J. Zhang, R.-G. Xiong, X.-T. Chen, Z. Xue, S.-M. Peng, X.-Z. You, *Organometallics* **2002**, *21*, 235−238. [6f] S. Sain, T. K. Maji, G. Mostafa, T.-H. Lu, M. Y. Chiang, N. R. Chaudhuri, *Polyhedron* **2002**, *21*, 2293−2299. [6g] J. Y. Lu, C. Norman, K. A. Abboud, A. Ison, *Inorg. Chem. Commun.* **2001**, *4*, 459−461. [6h] A. J. Blake, S. J. Hill, P. Hubberstey, W.-S. Li, *J. Chem. Soc., Dalton Trans.* **1997**, 913−914. [6i] K. Biradha, M. Fujita, *Chem. Commun.* **2001**, 15−16. [6j] R. H. Groeneman, L. R. MacGillivray, J. L. Atwood, *Chem. Commun.* **1998**, 2735−2736. [6k] J. T. Culp, J.-H. Park, M. W. Meisel, D. R. Talham, *Inorg. Chem.* **2003**, *42*, 2842−2848.

[7] M. C. Seidel, G. C. V. Tuyle, W. D. Weir, *J. Org. Chem.* **1970**, *35*, 1662−1664.

[8] *XSCANS, Release, 2.1*, Siemens Energy & Automation, Inc, Madison, Wisconsin, USA, **1995**.

[9] *SHELXTL 5.10*, Bruker Analytical X-ray Instruments Inc., Karlsruhe, Germany, **1997**.

Received February 8, 2004
Early View Article
Published Online October 1, 2004

